Engenharia Sanitária e Ambiental: Tecnologias para a Sustentabilidade 4

Alan Mario Zuffo
(Organizador)

Atena Editora
Ano 2019

Alan Mario Zuffo

(Organizador)

Engenharia Sanitária e Ambiental: Tecnologias para a Sustentabilidade 4

Atena Editora
2019

2019 *by Atena Editora*
Copyright © da Atena Editora
Editora Chefe: Profª Drª Antonella Carvalho de Oliveira
Diagramação e Edição de Arte: Lorena Prestes e Karine de Lima
Revisão: Os autores

Dados Internacionais de Catalogação na Publicação (CIP)
(eDOC BRASIL, Belo Horizonte/MG)

E57 Engenharia sanitária e ambiental [recurso eletrônico]: tecnologias para a sustentabilidade 4 / Organizador Alan Mario Zuffo. – Ponta Grossa (PR): Atena Editora, 2019. – (Engenharia Sanitária e Ambiental; v. 4)

Formato: PDF
Requisitos do sistema: Adobe Acrobat Reader.
Inclui bibliografia
ISBN 978-85-7247-252-4
DOI 10.22533/at.ed.524191104

1. Engenharia ambiental. 2. Engenharia sanitária. 3.Sustentabilidade. I. Zuffo, Alan Mario.

CDD 628

Elaborado por Maurício Amormino Júnior I CRB6/2422

APRESENTAÇÃO

A obra “Engenharia Sanitária e Ambiental Tecnologias para a Sustentabilidade” aborda uma série de livros de publicação da Atena Editora, em seu IV volume, apresenta, em seus 19 capítulos, os conhecimentos tecnológicos da engenharia sanitária e ambiental.

As Ciências estão globalizadas, englobam, atualmente, diversos campos em termos de pesquisas tecnológicas. Com o crescimento populacional e a demanda por alimentos tem contribuído para o aumento da poluição, por meio de problemas como assoreamento, drenagem, erosão e, a contaminação das águas pelos defensivos agrícolas. Tais fatos, podem ser minimizados por meio de estudos e tecnologias que visem acompanhar as alterações do meio ambiente pela ação antrópica. Portanto, para garantir a sustentabilidade do planeta é imprescindível o cuidado com o meio ambiente.

Este volume dedicado à diversas áreas de conhecimento trazem artigos alinhados com a Engenharia Sanitária e Ambiental Tecnologias para a Sustentabilidade. A sustentabilidade do planeta é possível devido o aprimoramento constante, com base em novos conhecimentos científicos.

Aos autores dos diversos capítulos, pela dedicação e esforços sem limites, que viabilizaram esta obra que retrata os recentes avanços científicos e tecnológicos, os agradecimentos do Organizador e da Atena Editora.

Por fim, esperamos que este livro possa colaborar e instigar mais estudantes e pesquisadores na constante busca de novas tecnologias para a Engenharia Sanitária e Ambiental, assim, garantir perspectivas de solução de problemas de poluição dos solos, rios, entre outros e, assim garantir para as atuais e futuras gerações a sustentabilidade.

Alan Mario Zuffo

SUMÁRIO

CAPÍTULO 7

QUANTUM DOTS FROM RENEWABLE PRECURSORS INCORPORATED AT ZINC OXIDE BY SONOCHEMICAL METHOD FOR PHOTOCATALYTIC PROPERTIES

Mayara Feliciano Gomes
Department of Chemical Engineering, Federal University of Rio Grande do Norte, Natal/RN, Brazil

Yara Feliciano Gomes
Department of Materials Engineering, Federal University of Rio Grande do Norte, Natal/RN, Brazil

André Luis Lopes Moriyama
Department of Chemical Engineering, Federal University of Rio Grande do Norte, Natal/RN, Brazil

Eduardo Lins de Barros Neto
Department of Chemical Engineering, Federal University of Rio Grande do Norte, Natal/RN, Brazil

Carlson Pereira de Souza
Department of Chemical Engineering, Federal University of Rio Grande do Norte, Natal/RN, Brazil

RESUMO: O estudo da dopagem com óxido de zinco (ZnO) na produção de materiais cerâmicos é amplamente utilizado como propriedade de fotocatalisadores e fotodegradação. Os pontos quânticos (QD_s) são nanopartículas semicondutoras que estão emergindo como uma nova classe de nanomateriais fluorescentes para aplicações ambientais. Neste artigo, através do método sonoquímico é proposta a incorporação de pontos quânticos de carbono (CQD_s) ao óxido de zinco. Os CQD_S são promissores nanomateriais, obtidos a partir de dois precursores renováveis que são materiais derivados de biomassa, da quitina (CH), quitosana (CS) e do grafite (G) como um terceiro material utilizado sintetizado pelo método de carbonização hidrotérmica. Neste trabalho, propôs-se a fazer um novo conjugado nano-fotocatalisador para o sistema ZnO / CQDs para garantir a estabilidade física e química, ter grupos de funcionalidades químicas, com grupos hidroxila, amino e carbonos (-OH, $-NH_2$, $-C_2$) que possibilitem aumentar a eficiência dos mesmos e serem potenciais substitutos dos fotocatalisadores tradicionais.

ABSTRACT: The study of zinc oxide (ZnO) doping in the production of ceramic materials is widely used as photocatalyst and photodegradation property. Quantum dots (QDs) are semiconductor nanoparticles that are emerging as a new class of fluorescent nanomaterials for environmental applications. In this paper, we are proposed for the incorporation of carbon quantum dots (CQD_s) into the zinc oxide by the sonochemical method. The CQD_S are promising nanomaterials, obtained from two renewable precursors, which are materials derived from biomass, as chitin (CH), chitosan (CS) and graphite (G) this as a third material used synthesized by the hydrothermal

carbonization method. In this work, proposed to make a conjugate novel nano-photocatalysts based on ZnO / CQD_s In order to ensure physical and chemical stability, have chemical functionalities groups, with hydroxyl groups, amino and carbons (-OH, $-NH_2$, $-C_2$), to investigate the possibility of increasing the efficiency of the same and potential substitutes for traditional photocatalysts.
KEYWORDS: sonochemical method, chitosan, quantum dots, carbonization hydrtothermal, fotocatalise

1 I INTRODUCTION

Studies using nanostructures zinc oxide háve been intensively investigated for production of ceramic materials have a variety of practical applications, especially the search for doping with elements that combined can be used in improvements in these applications as used for the rare earth elements. Doping of nanostructures using zinc oxide (ZnO) have interest to a variety of optical applications and potential material for high power laser, diode light, etc. and due to it is extensive range of applications such as sensors, LEDs (diodes in very high storage capacity, photocatalysis, among others investigated by (Chen et al, 2011) and (Gomes et al, 2016) and (Jung et al, 2012) have been extensively studied by (GONÇALVEs et al, 2002) as (PHURUANGRAT et al, 2014) and (GUO et al, 2011). Currently ZnO has been widely used as photocatalyst and photodegradation properties according to (CHEN et al, 2009), (WU et al, 2011), (FAISAL et al, 2013), (OLIVEIRA et al, 2006), (ESPINOSA et al, 2000), (SIN J-C et al, 2014) and (KUMAR et al, 2015).

Quantum dots (QDs) are semiconductor nanoparticles that are emerging as a new class of fluorescent nanomaterials for environmental applications as reported by (REZAEI et al, 2013), (SHEN et al, 2008), (ALAMO-NOLE et al, 2013), (SOLTANI et al , 2012), (MANSUR et al, 2014) and (JAVED et al. 2011). The semiconductor nanocrystals known as carbon quantum dots (CQDs) as demonstrated by (KUMARI et al, 2014), (SHARSHIR et al, 2017), (MANGAYIL et al, 2015), (NOVAKOVIĆ et al, 2008) and (ÖZDEMIR et al, 2011) which have physico-chemical, electronic, magnetic and optical properties, have recently emerging as a new class of fluorescent nanomaterials for environmental applications as noticed by (SAILIN et al, 2017) and (WANG et al, 2017). The CQDs must be water-soluble, biodegradable, non-toxic and have photoactivities of the conjugates for environmental applications as reported by (ULLAH et al, 2008). Due to these characteristics, they are proposed to improve properties in di□erent fields such as potential substitutes for traditional photocatalysts. Hydrothermal carbonization (HTC) is frequently used to synthesize CQDs because this method is considered as eco-friendly with great production viability and low cost. Os CQDs from two renewable precursors which are biomass-derived materials namely chitin (CH), chitosan (CS), and graphite (G) as a third material vem features such as biocompatibility, non-toxicity and being eco-friendly by (SIVAKUMAR et al, 2015) and (RAJABI et al, 2013). The

graphite (G) form of these nanoparticles shows desired properties such as high thermal conductivity, low cost and high solar absorptivity as compared with most of the other nanomaterials. (VILLAROEL et al, 2014)

Several routes for ZnO preparation with nanostructures doped with rare earth elements have been reported by (ALAMO-NOLE et al, 2013), (SOLTANI et al , 2012) abd (MANSUR et al, 2014), including methods as hydrothermal, magnetic spray deposition, pulsed laser deposition, photolithography and wet chemical recording by (JAVED et al. 2011) and (KUMARI et al, 2014). However, for this study we investigate the process of the sonochemichal method for incorpared quantun dots the structure of zinc oxide. This method have been advantageous because easy process, low cost, lower temperature and greater control of morphology by (SHARSHIR et al, 2017) and (MANGAYIL et al, 2015).

The sonochemical method allows the preparation of a wide variety of materials, including nanostructured. The d ultrasonic radiation present frequency higher than those detectable by the human ear, above 20 KHz. The sonochemical method have interations into the chemical and physical reactions of the particles do not result only from the interaction between the sound waves and the solution, they result mainly from the effect of acoustic cavitation, formation, growth and implosion of bubbles at localized points, increasing local temperature and pressure in a short time interval. This synthesis (sonochemical method) irradiation was employed by using a high intensity ultrasonic, the mixture transferred to a collecting cup which was adapted to be used in the sonochemical, the prepared colloidal suspensions will be processed in a cavitational ultrasonic waveform by the formation and collapse of microbubbles, these generated cavitations are responsible by the observed chemical effects and are produced by the subjection of a liquid to the ultrasonic energy that can oscillate between stable or unstable and are mostly responsible for the effects on the chemical reactions by (NOVAKOVIĆ et al, 2008) and (ÖZDEMIR et al, 2011)

In this work we report the study of conjugate novel nano-photocatalysts based on ZnO/CQDs In order to ensure a physical and chemical stability, have groups chemical functionalities, with hydroxyl groups (-OH) and amino (-NH_2), carbons (-C_2) to investigate the possibility of increase the efficiency of the same with and potential substitutes for traditional photocatalysts (YANG, YUNHUA, et al, 2012).

2 I EXPERIMENTAL SECTION

2.1 Synthesis processes

Using the sonochemical method, ZnO powders incorporated with CQDs from renewable precursors were obtained. For this synthesis, first were obtained the zinc oxide using the zinc nitrate ($Zn(NO_3)_2$) pure were dissolved in 80 mL deionized water under constant stirring. The zinc ions were added stoichiometric. The pH of the solution

was adjusted to 10 by adding NH_4OH, and the mixture was then transferred to a exposed to high-intensity ultrasonic irradiation (Branson Digital Sonifier) in a continuous mode with amplitudes 60% used time of 15 minutes min duration with temperature at 100° C, the final product a whiten power was obtained this product was separated by centrifugation, washed with deionized water and ethanol, and dried at 100 °C in air.

For synthesis of CQDs used are derived from biomass precursors chitin, chitosan and graphite were dissolved in ethanol (20 mL) and placed in Teflon-lined, hydrothermal reactor at 200°C for 6h. The light brown solution obtained was centrifuged at 10000 rpm for 10 min to remove the solution containing fluorescent CQDs from the solid black precipitate and with a photoluminescence quantum yield (F) of CQDs was determined following the procedure by using quinine sulfate as a reference (Sahu et al,2012).

After were obtained ZnO powders incorporated with CQDs from renewable precursors were dissolved in 80 mL deionized water under constant stirring and the mixture was then transferred to a exposed to high-intensity ultrasonic irradiation (Branson Digital Sonifier) in a continuous mode with amplitudes 60% used time of 15 minutes duration. The mixture transferred to a collecting cup which was adapted to be used in the sonochemical, the prepared colloidal suspensions was processed in a cavitational ultrasonic waveform by the formation and collapse of microbubbles, these generated cavitations are responsible by the observed chemical effects and are produced by the subjection of a liquid to the ultrasonic energy that can oscillate between stable or unstable and are mostly responsible for the effects on the chemical reactions by (NOVAKOVIĆ et al, 2008) and (ÖZDEMIR et al, 2011)

The final product a whiten power was obtained this product was separated by centrifugation, washed with deionized water and ethanol, and dried at 100 °C in air. The white powder obtained through the sonochemical synthesis were deagglomerated in an agate mortar and thus resulting in obtaining post-homogeneous and fine for characterization. The sonochemical synthesis irradiation was employed by using a high intensity ultrasonic.

2.2 Photocatalysis experiments

The photocatalytic degradation experiment was performed in a box containing a glass with lamps mounted horizontally, this being the source of radiation. Before going to degradation box, 0.05 g of powders was added in a 50 mL solution of methylene blue and was kept stirred for 15 min on a magnetic stirrer; thereafter, ´~ same solution was maintained under stirring in an ultrasound for the same period of time. Samples were with drawn at intervals of 30 min and then centrifuged before analysis. The measure much of methylene blue was degraded, UV–Vis spectrophotometer was used, which analyzed maximum absorption (MA) level at 664 nm, corresponding to its wavelength of maximum absorption, these percentages of material degradation efficiency were analyzed**.** Using the Tauc relation (TAUC et al, 1972) extracted from the UV–vis spectra

were determined the optical band gap (absorbance onset) and the blue-shift from the absorption coefficient data as a function of the wavelength.

2.3 Characterization

The structure of the crystalline phases in the calcined powders was investigated by X-ray diffraction (XRD) using a Rigaku MiniFlex II diffractometer with CuKα radiation (λ = 1.5418Å). For the phase identification, the measurements were carried out in the range of 2θ within 10° to 90° and the step speed of 0.02º/ min with fixed time of 2 s.

The lattice parameters and position were determined by means of the Rietveld refinement method and were analyzed by the Structure Analysis System (GSAS) program with the EXPGUI graphical interface program and the lattice parameters and atomic positions obtained were used to model these unit cells using the Visualization for Electronic and Structural Analysis (VESTA) program, version 3.1.2.

The values of the crystallite size and average strain value were obtained, using the Scherrer equation, which are related to the volume-weighted crystallite size, (D) to the integral width (taken on a 20 scale) of the size broadened profile. By applying some weighted average strain value, the approximate value is obtained from the integral width of the extended strain profile, and it was obtained by the GSAS program, as represented in Equation (1) and (2) (WANG et al, 2017).

$$< D >_v = \lambda/(\beta^S \cos\theta) \quad (1)$$

$$\tilde{e} = \frac{1}{4}\beta^D \cot\theta \quad (2)$$

The samples were investigated by EDS spectroscopy using a field-emission gun scanning electron microscopy (FEG-SEM; Carl Zeiss, Supra 35-VP Model, Germany) operated at 14 kV. The wavelengths related to higher absorbance peak of the degradation of Zinc Oxide obtained by analysis of the UV–Vis spectroscopy were the response variables with the percentage of doping efficiency values by (ULLAH et al, 2008), (SIVAKUMAR et al, 2015) and (RAJABI et al, 2013). The PL spectra were recorded at an excitation wavelength of 350 nm at room temperature using a photoluminescence spectrometer Hamatsu R446 “lock in” SR-530.

3 I RESULTS AND DISCUSSION

The patterns of the X-ray diffraction of the samples synthesized by the sonochemical method are shown in Figure. 1. The XRD was used to verify the crystal structure and purity of the samples. Figure 1 presents the X-ray diffractograms of ZnO/ CQDs powders as response surface obtained according to the sonochemical method,

showing its crystallization with the presence of phase that identifies the formation of zinc oxide having the wurtzite type hexagonal structure. All the diffraction peaks can be indexed to the hexagonal structure of ZnO (JCPDS No 36-1451) having the P63cm space group (PHURUANGRAT et al, 2014). This was verified by standard XRD crystallographic record with the JCPDS No. 36-1451 through the search-match program, which indicated the incorporation of quantum dots at zinc oxide network through observing the formation of a single phase crystal structure for pure ZnO and ZnO with increasing quantum dots, ZnO/CQDs as shown Figure 1 and in detail the structure CQDs when don't have increasing into zinc oxide (fig.1b).

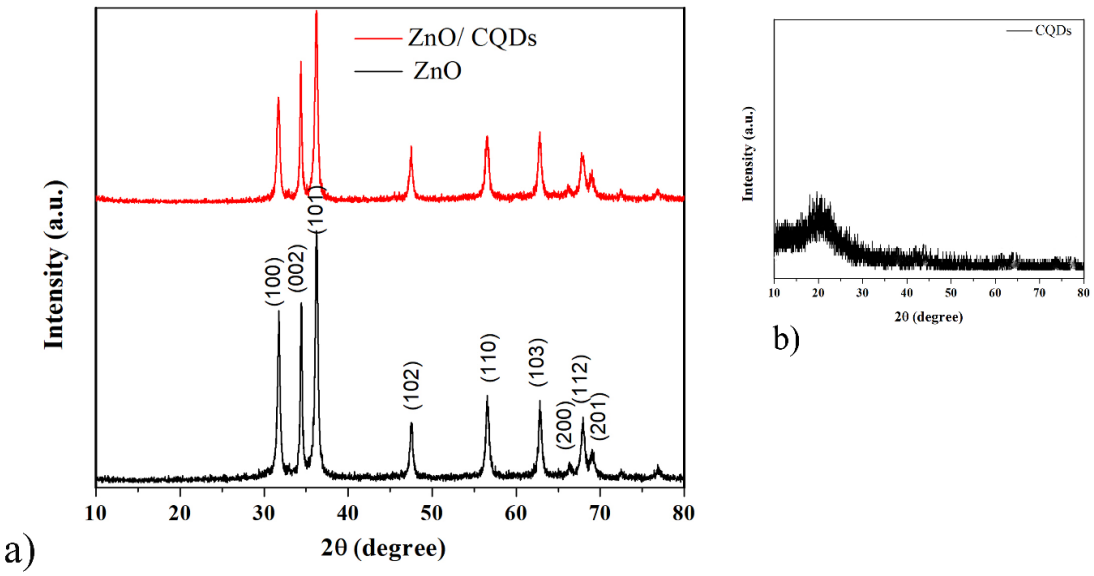

Figure 1. X-ray diffraction diagram of powder ZnO/CQDs samples prepared with sonochemical method and detail sample CQDs.

The crystallization has been the presence of peaks that vary from a lower intensity to a higher intensity with the single phase of ZnO, as can been observed through the card JCPDS 36-1451 and this is due to the increase in temperature in which at 100 ºC, there are small peaks up to 100 ° C with higher peak intensities, these peaks acquire a higher intensity of crystallization as shown in Figure 1. The peaks revealed that the prepared particles have an increase in intensity of 2θ when the ZnO is replaced and different the structure the CQDs when don't have incorporated zinc oxide. The results of the Network Parameters and Unit Cell Volumes have their values confirmed by the values previously reported (SHEN et al, 2008) and thus, they have similar values when a = 6.25 (Å) and c = 12.16 (Å). Thus, observing Table 1 confirmed the structure values through the use of the Rietveld refinement method by (MANSUR et al, 2014) and (JAVED et al. 2011)

The Figure 1 shown diffractograms with the JCPDS No. 36-1451 where a = 3.25 Å, c = 5.20 Å as according with the literature and peaks (100), (002), (101), (110), (103) and (112) correspondents principals peaks of ZnO. The crystalline of material

as observed as compared when incorporated the quantum dots, assumed the same parameter of ZnO.

XRD of the samples of the CQDs are shown in Figure 1 (b), all the patterns were same of the main structure with an sp^2 set with stacking faults based on a wide 002 peak at approximately 2θ = 20.6 °, and no other peak was detected, thus confirming the amorphous nature of all, as studied for quantum dots of biomass derivatives (chitin and chitosan) the results pattern of the XRD of the graphite showing the (002) higher peaks revealed centered around 2θ = 21.25 ° confirmed with the structures similar to graphite as studied previously (FRADE et al, 2012).

The Figure 1 shown diffractograms with the crystalline peaks of the material incorporated by the dots, Zno / CQDs, the characteristic peaks of the single phase of Zno were maintained and thus identified the doping of the material.

The XRD data were processed by Rietveld refinement. The Rietveld refinement method by (PHURUANGRAT et al, 2014) and (FRADE et al, 2012) was used to explain the possible differences in the structural arrangements induced by the processing of the ZnO particles. The Structure Analysis System (GSAS) program with the EXPGUI program with the graphical interface by (MONTERO-MUÑOZ et al, 2018) and (KEIJSER et al, 1983) was used to perform the refinement. The refined parameters were: scaling factor and phase fraction; background, were used to model these unit cells using the Visualization for Electronic and Structural Analysis (VESTA) program, version 3.1.2. was modeled using a displaced Chebyshev polynomial function; peak shape, which was modeled using Thomson-Cox-Hasting pseudo-Voigt; change in lattice constants; fractional atomic coordinates; and isotropic thermal parameters. The results of the Rietveld refinement are shown Figure 2.

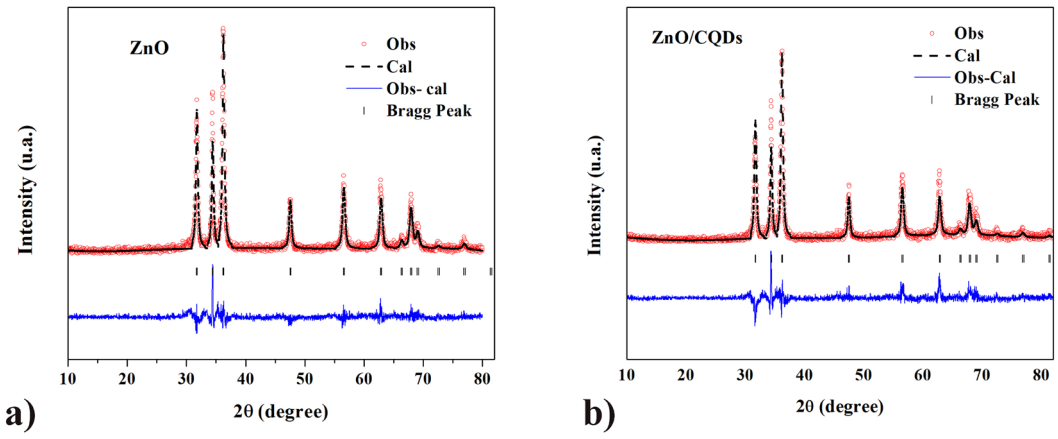

Figure 2. Rietveld refinement plot of sample of ZnO and ZnO/CQDs prepared with sonochemical method at a) refinement plot of sample ZnO and b) refinement plot sample of ZnO/CQDs.

Figure 2 shows the corresponding refinement at a temperature until 100 ° C with the ZnO increasing quantum dots. The appearance of characteristic diffraction peaks for a pure ZnO sample corresponding to (1 0 0), (0 0 2), (1 0 1), (1 0 2), (1 1 0), (1 0

3) and (11 2) planes is in good agreement with the standard XRD peaks of crystalline bulk ZnO with hexagonal wurtzite structure JCPDS No. 36–1451, a = 3.2501 Å , c = 5.2071 Å, space group: P63mc . The gradual changes of the FWHM of characteristic peak (002) is shown as an inset to show the refinement of evolved structure, at 1000 ºC, the best result is obvious from the spectrum by (SALEM et al, 2018) and (SABIR et al, 2014).

Table 1 showed the Rietveld refinement parameters, crystallite size, and degree of crystallinity. The quality of the refinement was quantified by the corresponding pre-determined values: profile residual R_p, weighted profile residual R_{wp} and adjustment quality χ^2. In table 1, it was verified that the lattice parameters and unit cell volumes are very close to the values recently published in the literature (SARIC et al, 2017), considering the crystallite size the effects of zinc oxide on the morphology quantum dots, the particle sizes, purity and the phase of ZnO samples have been investigated. The results have been listed in Table 1 according to (KAHOULI et al, 2015) and (MIRZAEI et al, 2017).

Compounds	ZnO	ZnO/CQDs
Crystal System	Hexagonal	Hexagonal
Space Group	P63cm	P63cm
A	3.25161	3.25161
B	3.25161	3.25161
C	5.20689	5.20689
V(Å³)	47.67	47.80
X²	1.36	1.41
Rwp (%)	24.45	28.67
Rp (%)	17.32	20.19

Table 1. Structural Parameters for ZnO and ZnO/CQDs from Rietvield refinement of powders X –ray diffraction data.

The quantification of these parameters was made through the experimental XRD and it was carried out in the P63mc space group using the structural parameters for ZnO as the initial model. ZnO / CQDs refining, the atomic positions were accurately

fasten for all cell samples, and these values were assigned by Vesta program for the structure formation. Also, the doping of CQDs and the temperature used caused the formation or reduction of structural defects: oxygen vacancies, distortion on the bonds, stresses and strains on the crystalline lattice. The values of the adjustment parameters (R_{wnb}, R_b, R_{exp}, R_w, and χ^2) suggest that the refinement results are reliable as shown in Table 2 according to (NGOC-TRAM LE et al, 2018), (SAADELDIN et al, 2018) and (KIMIAGAR et al, 2018)

(a)Atom[a]	X	y	z	occupancy	B	Site	Sym.
Zn_1	0.33333	0.66667	0.00661	1.000	0.629	2b	3.m
O_1	0.33333	0.66667	0.38133	1.000	0.629	2b	3m
b)Atoms[b]							
Zn_1	0.33366	0.66667	0.10839	0.998	0.133	12d	1
O_1	0.33298	0.66667	0.49121	0.992	3.795	12d	1
CQDs	0.00000	0.00000	-0.06518	0.992	75.565	2a	3m.

[a]ZnO synthesized by Sonochemical method.

[b]ZnO/CQDs synthesized by Sonochemical method.

Table 2. Atomic coordinate obtained experimentally from the structural of ZnO and ZnO/CQDs refinement by the Rietveld method and theoretically calculated with an electronic and structural analysis Vesta program.

These unit cells were modeled using the Visualization for Electronic and Structural Analysis (VESTA) program, version 3.1.2, for Windows as shown in Figure 3 for doping ZnO/CQDs all at 100 ºC temperature (GHAMSARI et al, 2019). Therefore, the SEM results indicated that the CQDs in the ZnO structure were adequately stabilized by the functional groups (-NH, -CC, -O), which is in reasonable agreement with the values obtained in the x-ray shown in Figure 1. The fluorescent quantum yield was thus calculated to be 17.1% using quinine sulfate as a reference (Sahu et al, 2012).

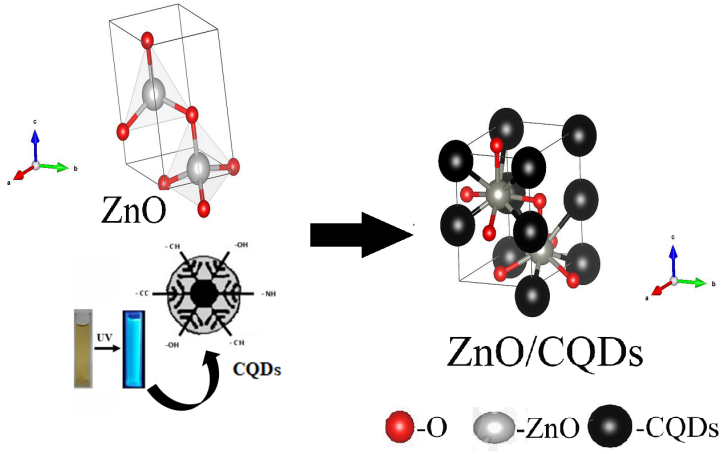

Figure 3. Schematic representation of the structure corresponding to sample of ZnO and ZnO/ CQDs prepared with sonochemical method at a) structure of ZnO .

The SEM/ EDS mapping the samples are as shown in the Figure 4 (a-h), the micrograph of ZnO shown at Fig. 4 (a, b and c) as observed hexagonal wurtzite structure type flower. The analysis of prepared samples identified the ZnO at hexagonal structure in the homogeny distribution for samples as shown Figure 4 (h). The CQD_s via sonochemical method using temperature at 100 ºC can been observed as shown the micrograph for the system ZnO/CQD_s at Fig. 4 (d, e and f) observed hexagonal wurtzite structure type roods and the distribution of the atoms for samples as shown the Figure 4 (g) confirmed the presence different functional groups (such as carboxylic groups, hydroxyl groups, amines, amides), attributed to the stretching of -CH, -NH and –OH, -CO, -CC and -CH, respectively, for formulation CQDs (Yang et al, 2012). The particles of ZnO-CQDs, provides a better defined as roods different to that morphology of pure ZnO as type flower, but the system of ZnO-CQDs a greater amount of clusters and larger particle size (THABIT et al, 2018).

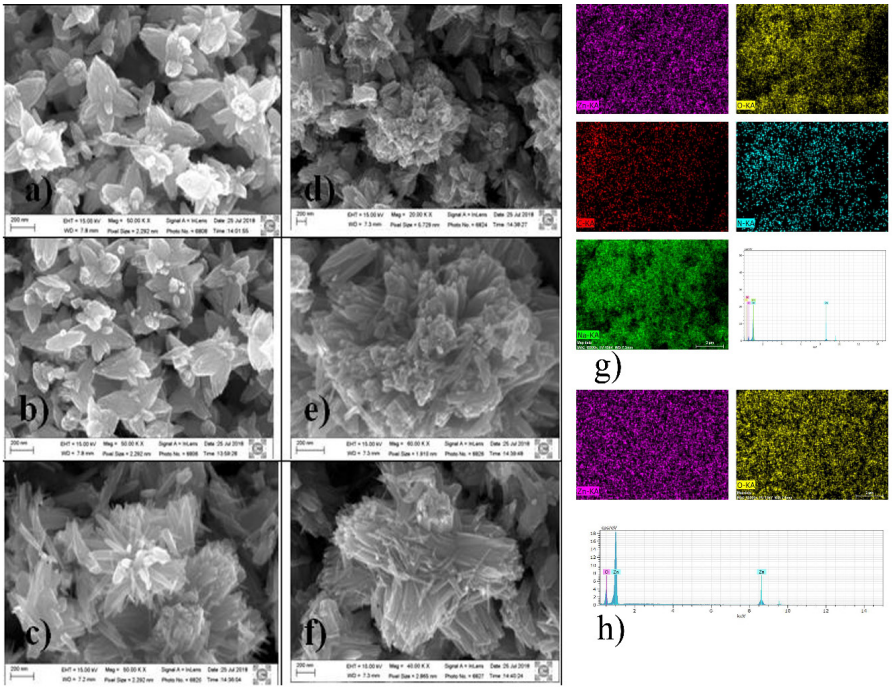

Figure 4. EDS mapping of the synthesized powder ZnO/CQDs samples prepared with sonochemical method. a) Zno samples and b) ZnO/CQDs samples.

Figure 5 showed the optical properties of the pure ZnO, and ZnO / CQDs were obtained by sonochemical with the PL measurement, respectively. The effect of adsorption on the PL emission properties of ZnO has been well studied in literatures by (TAUC et al, 1972), (JUNG et al , 2011) and (FANG et al , 2018).

The photoluminescence spectra of the ZnO pure and ZnO / CQDs system of nanoparticles collected at room temperature (RT). Figure 5 shows the PL of the CQDs is the emission starts at 477 nm and ends at 648 nm. The difference in PL intensity between ZnO pure and ZnO / CQDs is attributed to the presence of surface groups (O-H, N-H, and C = O) of carbon quantum dots as reported by (JUNG et al , 2011) and (BRISCOE et al, 2015) are influenced for values band gap.

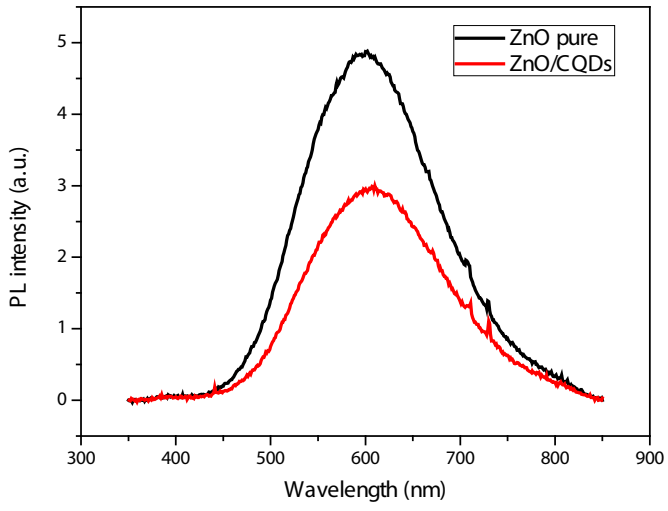

Fig.5. (a) Optical band gap plot using Tauc equation of the ZnO pure and (b) the ZnO/ CQDS.

Figure 6 shows the band gap energy values of the ZnO semiconductor is about 3.29 eV and with the addition of the CQDs that has band gap energy of 3.15 eV, the value of the bulk has the decrease of ZnO / CQDs with a value of 3.23 eV. Therefore the particle size of ZnO and ZnO / CQDS under study in this work is small enough to make the particle surfaces have a dominant role in the PL process.

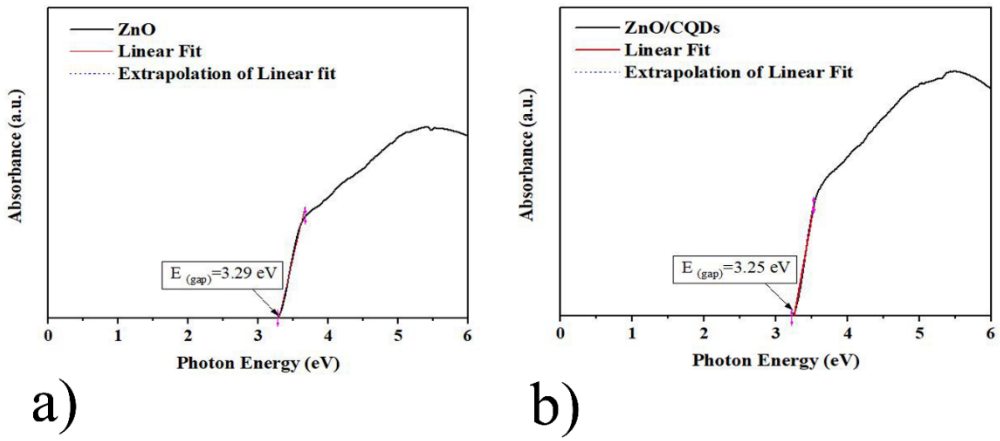

Figure 6. Degradation efficiency versus time of sample ZnO –CQDs particles obtained using sonochemical method at 100°C, respectively for ZnO and ZnO-CQDs.

Figure 7 shows the increased photocatalytic activity of ZnO ZnO / CQDs system nanostructures can be attributed to increase the CQDs into the structure ZnO. However, these ions can act as a center of recombination between the electron excited during the photocatalysis processes by (OLIVEIRA et al, 2006) and (TAUC et al, 1972).

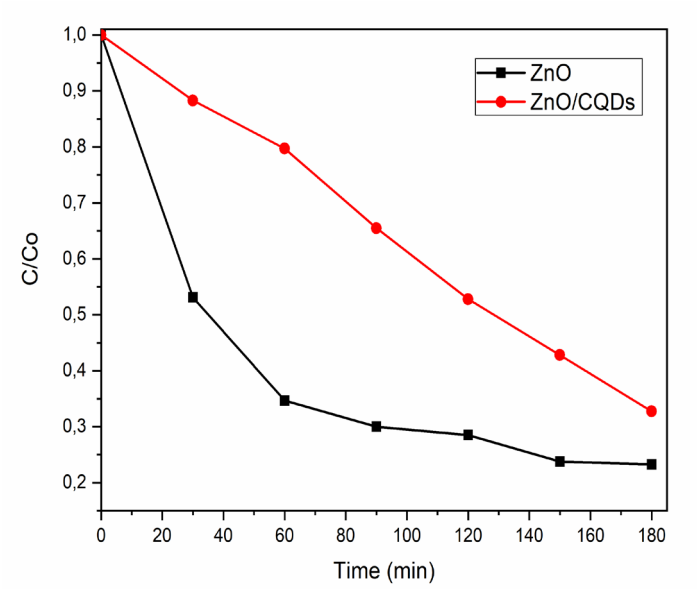

The effect the photocatalytic of ZnO has been reported studied in literatures by (KIMIAGAR et al, 2018), (THABIT et al ,2018) and (FANG et al , 2018) so the effect the photocatalytic for ZnO above 70% this case the ZnO for this study as shown in Figure 7

obtained a degradation of 74% and when including CQDs as shown had a degradation of 70% with a significant response to the doping of the CQDs in the zinc oxide structure.

4 I CONCLUSION

The study of Zinc oxide included CQDs into the system by sonochemical method was analyzed. The low temperature at 100 °C was efficiency the formation of a single phase crystal structure for increasing CQDs the peaks that correlate to the wurtzite ZnO (JCPDS = 36-1451) at 31.77, 34.48 and 36.50 that correlate to the ZnO (100), (002) and (101) planes for the samples CQDs. The quality of the refinement was quantified by the corresponding pre-determined values: profile residual R_p, weighted profile residual R_{wp} and adjustment quality χ^2 has been studied at literature and confirmed in this study. The SEM shows that the samples of pure ZnO have large amounts of ZnO with similar nanoparticles with flower shape. Among the particles of ZnO/CQD_s, provides a better defined as roods different to that morphology of pure ZnO, but a greater amount of clusters and larger particle size. The photocatalytic activity as observed the efficiency degradation of ZnO pure and the included CQDs was efficient in the degradation of the material with 70% efficiency. The gap band Eg = 3.29 eV for ZnO and with CQDs the band gap Eg = 3.25 eV. The investigated the possibility of increasing the efficiency of the same and potential substitutes for traditional photocatalysts.

5 I ACKNOWLEDGEMENTS

The authors thank the financial support of the Brazilian research financing institutions: CNPq and CAPES.

REFERENCES

A.SARIC, M. Gotic, G. Stefanic, G. Drazic.Synthesis of ZnO particles using water molecules generated in esterification reaction. Journal of Molecular Structure 2017, 1140: 12-18.

ALAMO-NOLE, L., Bailon-Ruiz S., Luna-Pineda T., Perales-Perezab O., Romana F.R., Photocatalytic activity of quantum dot–magnetite nanocomposites to degradeorganic dyes in the aqueous phase, J. Mater. Chem. A 1 (2013) 5509–5516.

BRISCOE, Joe, et al. Biomass-derived carbon quantum dot sensitizers for solid-state nanostructured solar cells. Angewandte Chemie International Edition 54.15 (2015) 4463-4468. https://doi.org/10.1002/anie.201409290.

CHEN S, Zhao W, Zhang S, et al. Preparation, characterization and photocatalytic activity of N-containing ZnO powder. Chem Eng J 2009, 148: 263–269.

CHEN XY, Fang F, Ng AMC, et al. Effect of doping precursors on the optical properties of Ce-doped ZnO nanorods. Thin Solid Films 2011, 520: 1125–1130.

ESPINOSA MM, Calil C Jr. Statistical fatigue experiment design in medium density fiberboard. Mat Res 2000, 3: 84–91.

FAISAL M, Ismail AA, Ibrahim AA, et al. Highly efficient photocatalyst based on Ce doped ZnO nanorods: Controllable synthesis and enhanced photocatalytic activity. Chem Eng J 2013, 229: 225–233.

GOMES, Y. F., Freitas, A. K., Nascimento, R. M., BOMIO, M. R. D.,PASKOCIMAS, C. A., MOTTA, F. V. Experimental statistic design applied for obtaining Zn:xCe by microwave-assisted hydrothermal method with photocatalytic property. Journal of Advanced Ceramics, 2016, 2: 103–110.

GONÇALVES AS, Lima SAM, Davolos MR. Gallium-doped zinc oxide prepared by the Pechini method. Eclética Química 2002, 27: 293–304.

GUANGANG WANG, Guangsheng Huang, Xiang Chen, Qianyuan Deng .Effects of Zn addition on the mechanical properties and texture of extruded Mg-Zn-Ca-Ce magnesium alloy sheets. Mat Sci Eng. 2017,705: 46-54.

GUO MY, Fung MK, Fang F, et al. ZnO and TiO2 1D nanostructures for photocatalytic applications. J Alloys Compd 2011, 509: 1328–1332.

H. A. THABIT, N. A. Kabir .The study of X-ray effect on structural, morphology and optical properties of ZnO nanopowder. Nuclear Inst. and Methods in Physics Research B 2018, 436: 278–284.

H. MIRZAEI, M. Darroudi. Zinc oxide nanoparticles: Biological synthesis and biomedical applications. Ceramics International 2017, 43: 907–914.

H.R. RAJABI, O. Khani, M. Shamsipur, V. Vatanpour, High-performance pure andFe^{3+}ion doped ZnS quantum dots as green nanophotocatalysts for the removalof malachite green under UV-light irradiation, J. Hazard. Mater. 250/251 (2013)370–378.

IQBAL, Javed et al. Adsorption of acid yellow dye on flakes of chitosan prepared from fishery wastes. Arabian Journal of Chemistry, v. 4, n. 4 (2011) p. 389-395.

LV, J., & Fang, M. (2018). Photoluminescence study of interstitial oxygen defects in ZnO nanostructures. *Materials Letters*, *218*, 18-21.

J. TAUC, A. Menth, States in the gap, J. Non-Cryst. Solids 8/10 (1972) 569–585.

JUNG Y-I, Noh B-Y, Lee Y-S, et al. Visible emission from Ce-doped ZnO nanorods grown by hydrothermal method without a post thermal annealing process. Nanoscale Res Lett 2012, 7: 43.

JUNG, M. H., & Lee, H. (2011). Selective patterning of ZnO nanorods on silicon substrates using nanoimprint lithography. Nanoscale research letters, 6(1), 159.

KEIJSER, TH. H, Mittemeijer, E.J., Rozendaa, H. C. E, .The Determination of Crystallite-Size and Lattice-Strain Parameters in Conjunction with the Profile-Refinement Method for the Determination of Crystal Structures, J. Appl. Cryst. 16 (1983) 309-316.

KUMAR R, Umar A, Kumar G, et al. Ce-doped ZnO nanoparticles for efficient photocatalytic degradation of direct red-23 dye. Ceram Int 2015, 41: 7773–7782.

KUMARI, Suneeta; RATH, Pradip Kumar. Extraction and characterization of chitin and chitosan from (Labeo rohit) fish scales. Procedia Materials Science, v. 6 (2014)

M. KAHOULI, A. Barhoumi, A. Bouzid, A. Al-Hajry, S. Guermazi. Structural and optical properties of ZnO nanoparticles prepared by direct precipitation method. Superlattices and Microstructures 2015, 85: 7–23.

M. MONTERO-MUÑOZ, J.E. Ramos-Ibarra, J. E. Rodríguez-Páez, M. D. Teodoro, G. E. Marques, A. R. Sanabria, P. C. Cajas, C. A. Páez, B. Heinrichs, J. A.H. Coaquira. Role of defects on the enhancement of the photocatalytic response of ZnO nanostructures. Applied Surface Science 2018, 448: 646–654.

M. SALEM, S. Akir, I. Massoudi, Y. Litaiem, M. Gaidi, K. Khirouni. Photoelectrochemical and optical properties tuning of graphene-ZnOnanocomposites. Journal of Alloys and Compounds 2018, 767: 982-987.

M. SASANI GHAMSARI, S. Alamdari, D. Razzaghi, M. Arshadi Pirlar. ZnO nanocrystals with narrow-band blue emission. Journal of Luminescence 2019, 205: 508–518.

M.M. SAADELDIN, O. A. Desouky, M. Ibrahim, G.E. Khalil, M.Y. Helali. Investigation of structural and electrical properties of ZnO varistor samples doped with different additives. NRIAG Journal of Astronomy and Geophysics 2018, In press, corrected proof, Available online 4 July 2018.

MANGAYIL R, Aho T, Karp M, et al. Improved bioconversion of crude glycerol to hydrogen by statistical optimization of media components. Renew Energ 2015, 75: 583–589.

MANSUR, Alexandra AP, et al. “Green” colloidal ZnS quantum dots/chitosan nano-photocatalysts for advanced oxidation processes: study of the photodegradation of organic dye pollutants. Applied Catalysis B: Environmental, 2014, 158: 269-279.

Nanostructures. Materials Letters 2018, 218: 18–21.

NGOC-TRAM LE, J. Myrick, T. Seigle, P.T. Huynh, S. Krishnan. Mapping electrospray modes and droplet size distributions for chitosan solutions in unentangled and entangled concentration regimes. Advanced Powder Technology 2018, In Press, Uncorrected Proof, Available online 17 October 2018.

NOVAKOVIĆ T, Rožić L, Petrović S, et al. Synthesis and characterization of acid-activated Serbian smectite clays obtained by statistically designed experiments. Chem Eng J 2008, 137: 436–442.

OLIVEIRA TF, Avillez RR, Epprecht EK, et al. Evaluation via multivariate techniques of scale factor variability in the Rietveld method applied to quantitative phase analysis with X-ray powder diffraction. Mat Res 2006, 9: 369–374.

ÖZDEMIR E, Duranoğlu D, Beker Ü, et al. Process optimization for Cr(VI) adsorption onto activated carbons by experimental design. Chem Eng J 2011, 172: 207– 218. p. 482-489.

PHURUANGRAT A, Yayapao O, Thongtem T, et al. Preparation, characterization and photocatalytic properties of Ho doped ZnO nanostructures synthesized by sonochemical method. Superlattice Microst 2014, 67: 118–126.

PHURUANGRAT A, Yayapao O, Thongtem T, et al. Preparation, characterization and photocatalytic properties of Ho doped ZnO nanostructures synthesized by sonochemical method.Superlattice Microst 2014, 67: 118–126.

REZAEI M, Habibi-Yangjeh A. Microwave-assisted preparation of Ce-doped ZnO nanostructures as an efficient photocatalyst. 2013. Available at http://agris.fao.org/ agris-search/search. do?recordID=US201500026750.

S. KIMIAGAR, S. Safa, S. Gharedaghi. N-doped graphene: a trustful additive concerning to the photocatalytic properties of ZnO. Optik 2018, 174: 163- 166.

S. SABIR, M. Arshad, S. Khalil Chaudhari. Zinc Oxide Nanoparticles for Revolutionizing Agriculture: Synthesis and Applications. The Scientific World Journal 2014, Article ID 925494.

SAHU, S., Behera, B., Maiti, T. K., & Mohapatra, S. (2012). Simple one-step synthesis of highly

luminescent carbon dots from orange juice: application as excellent bio-imaging agents. Chemical Communications, *48*(70), 8835-8837.

SAILIN, Fan, Chang junWu, Ya Liu, HaoTu, Xuping Su, Jianhua Wang .600 and 450 °C isothermal sections of the Zn–Ce–Ti system. J Alloys Compounds, 2017, 709: 842-849.

SHARSHIR, S. W., Peng, G., Wu, L., Essa, F. A., Kabeel, A. E., & Yang, N. The effects of flake graphite nanoparticles, phase change material, and film cooling on the solar still performance. Applied Energy, 191 (2017) 358-366.

SHEN W, Li Z, Wang H, et al. Photocatalytic degradation for methylene blue using zinc oxide prepared by codeposition and sol–gel methods. J Hazard Mater 2008, 152: 172–175.

SIN J-C, Lam S-M, Lee K-T, et al. Preparation of rare earth-doped ZnO hierarchical micro/nanospheres and their enhanced photocatalytic activity under visible light irradiation. Ceram Int 2014, 40: 5431–5440.

SIVAKUMAR, p. Nayak, p.k., Markovsky, b., Aurbach, d., G1edanken, a. Sonochemical Syntheses of $LiNi_{0.5}Mn_{1.5}O_4$ and its Eletrochemical performace as a cathode material for 5V Li-ion batteries. Ultrasonics Sonochemistry 26 (2015) 332-339.

SOLTANI, N., Saion, E., Hussein, M.Z., Erfani, M., Abedini, A. G. Bahmanrokh, M.Navasery, P. Vaziri, Visible light-induced degradation of methylene blue in thepresence of photocatalytic ZnS and CdS nanoparticles, Int. J. Mol. Sci. 13 (2012)12242–12258.

T. FRADE, M.E. Melo Jorge, A. Gomes. One-dimensional ZnO nanostructured films: Effect of oxide nanoparticles. Materials letters 2012, 82: 13-15.

ULLAH, R., Dutta, J., Photocatalytic degradation of organic dyes with manganesedoped ZnO nanoparticles, J. Hazard. Mater. 156 (2008) 194–200.

VILLAROEL, Erica, agredo, javier silva-, petrier, christian, taborda, gonzalo, torres-palma , ricardo a. Ultrasonic degradation of acetaminophen in water: effect of sonochemical parameters and water matrix. Ultrasonics sonochemistry 21 (2014) 1763–1769.

WU C, Shen L, Zhang Y-C, et al. Solvothermal synthesis of Cr-doped ZnO nanowires with visible light-driven photocatalytic activity. Mater Lett 2011, 65: 1794–1796.

YANG, Yunhua, et al. One-step synthesis of amino-functionalized fluorescent carbon nanoparticles by hydrothermal carbonization of chitosan. Chemical Communications, 2012, 48.3: 380-382.

SOBRE O ORGANIZADOR

Alan Mario Zuffo - Engenheiro Agrônomo (Universidade do Estado de Mato Grosso – UNEMAT/2010), Mestre em Agronomia – Produção Vegetal (Universidade Federal do Piauí – UFPI/2013), Doutor em Agronomia – Produção Vegetal (Universidade Federal de Lavras – UFLA/2016). Atualmente, é professor visitante na Universidade Federal do Mato Grosso do Sul – UFMS no Campus Chapadão do Sul. Tem experiência na área de Agronomia – Agricultura, com ênfase em fisiologia das plantas cultivadas e manejo da fertilidade do solo, atuando principalmente nas culturas de soja, milho, feijão, arroz, milheto, sorgo, plantas de cobertura e integração lavoura pecuária. E-mail para contato: alan_zuffo@hotmail.com

Agência Brasileira do ISBN
ISBN 978-85-7247-252-4